Clays and Clay Minerals, Vol. 68, No. 4:309–318, 2020

FABRICATION OF CERAMIC, HOLLOW-FIBER MEMBRANE: THE EFFECT OF BAUXITE CONTENT AND SINTERING TEMPERATURE

Nurul Jannah Ismail[1], Mohd Hafiz Dzarfan Othman[1]*, Suriani Abu Bakar[2], Juhana Jaafar[1], and Mukhlis A Rahman[1]

[1]Advanced Membrane Technology Research Centre (AMTEC), School of Chemical and Energy Engineering, Faculty of Engineering, Universiti Teknologi Malaysia, UTM, 81310 Johor Bahru, Johor, Malaysia

[2]Nanotechnology Research Centre, Faculty of Science and Mathematics, Universiti Pendidikan Sultan Idris, 35900 Tanjung Malim, Perak, Malaysia

Abstract—The negative effects of dye-contaminated wastewater on humans and the environment are well known, so the wastewater must be treated carefully before discharge into the environment. To overcome those impacts, the search for environmentally friendly and low-cost materials is essential, especially in developing countries The objective of the present study was to determine the feasibility of using bauxite from Malaysia as a new and efficient ceramic, hollow-fiber membrane for the degradation of reactive dyes in wastewater. A porous, hollow-fiber membrane was fabricated from bauxite (BHFM) using a phase-inversion technique, followed by sintering at various temperatures. The BHFM consisted of two types of voids, having either a finger-like or a sponge-like structure. As the sintering temperature was increased, the porosity of the BHFM decreased from 46.5 to 9.5%. The greatest mechanical strength of 308.1 MPa was achieved when the BHFM was loaded with 55 wt.% of bauxite and sintered at 1450°C. The remaining 45 wt.% consisted of solvent, polymer binder, and dispersant. The BHFM functioned well as a membrane for microfiltration and a support membrane for ultrafiltration. BHFM with loading of 45 wt.%, 50 wt.%, and 55 wt.% successfully eliminated 90%, 94%, and 98% of 10 ppm reactive dye (RB5) when sintered at the highest temperature.

Keywords—Bauxite · Hollow-fiber membrane · Mechanical properties · Sintering temperature · Ultrafiltration

INTRODUCTION

Ceramic, porous membranes have received significant attention recently due to their flexural structure, thermal stability, and good wettability. This type of membrane has become important in membrane reactors, absorbers, and bioceramics as well as in catalyst supports. Limitations in terms of the mechanical, thermal, and chemical resistance properties of polymeric membranes have led to emphasis on the utilization of ceramic membranes. These types of membranes are often relatively well defined, have a narrow pore-size distribution, and have significant porosity which allow a high water flux, superior layer separation, and high mechanical stability so they can be used under elevated applied pressures and in harsh chemical and thermal conditions. These characteristics extend their operational lifetime. Moreover, their hydrophobicity results in a greater flux at low pressures (Ma et al. 2010). The main drawbacks of ceramic membranes, however, has been the high cost of raw materials and the amount of energy required for the sintering process at >1600°C (Sabbatini et al. 2010). Thus, recent efforts have turned toward a search for less expensive methods and materials (Ebbesen et al. 2014), which in turn has led to increased interest in bauxite, a naturally occurring material rich in aluminum.

The reserves of bauxite are estimated to be ~55–75 billion tons worldwide, showing that it is abundant and available widely.

According to a previous study conducted by Ren et al. (2018), the quality of bauxite ore is variable, depending on the relative amounts of impurities and its refractoriness (resistance to decomposition by heat, pressure, or chemical attack up to 1770°C). Impurities include hematite (Fe), goethite (Fe), quartz (Si), and anatase and rutile (Ti) (Bauxite Index 2020). Upon heating, the quartz in the bauxite enables the formation of mullite, a chemically stable aluminosilicate, via a secondary mullitization reaction which later enhances the mechanical strength of the fabricated membrane. The composition of bauxite makes it ideal for use as a raw material for ceramic-membrane development.

There are four types of geometrical configuration of ceramic membranes: plate and frame (pillow-shaped), tubular, capillary, and hollow-fiber. Among these configurations, however, hollow-fiber membranes offer advantages such as large surface area per unit volume, good flow profiles through the hollow structure, and are suitable for use in existing reactors (Ren et al. 2018). Phase inversion is a chemical phenomenon exploited in the fabrication of artificial membranes. It is performed by removing the solvent from a liquid-polymer solution, leaving a porous, solid membrane. It is a method used commonly to form filtration membranes, which are typically formed using artificial polymers. The phase inversion method is heavily dependent on the type of polymer used and the solvent used to dissolve the polymer. Furthermore, the phase-inversion process used to develop this hollow-fiber membrane is cost-effective because the process is simple; no energy-intensive processes are required and only a small amount of additives is involved (Li et al. 2016). To date, the fabrication of

* E-mail address of corresponding author: hafiz@petroleum.utm.my

DOI: 10.1007/s42860-020-00076-8

Table 1. Composition for dope suspension

Material	Molecular formula		Bauxite loading (%)		
			45	50	55
Bauxite powder	Raw bauxite	$Al(OH)_3$	45.00 g	50.00 g	55.00 g
Polymer binder	Polyethersulfone (PES)	$C_{12}H_8SO_3$	5.63 g	6.25 g	6.88 g
Dispersant	Polyethyleneglycol 30-dipolyhydroxystearate (Arlacel P135)	PHS-PEO-PHS block copolymer	1.00 g	1.00 g	1.00 g
Solvent	N-methyl-2-pyrrolidone (NMP)	C_5H_9NO	48.38 g	42.75 g	37.12 g

hollow-fiber membranes utilizing cheap and abundant bauxite as the only material involved in phase inversion has rarely been reported (Meng et al. 2014).

A hollow-fiber structure has been selected as the configuration to be used in the present study because of its advantages for wastewater treatment, Thus, due to the aforementioned advantages of bauxite as a material for hollow-fiber membrane production, the objective of the present study was to develop asymmetrical, hydrophilic, hollow-fiber membranes, using raw bauxite as the starting material, and to discover the best combination of bauxite loading and sintering temperature for ultrafiltration applications.

EXPERIMENTAL PROCEDURE

Materials

Bauxite was obtained as a raw ore from Kuantan, Pahang, Malaysia (Aras Kuasa Sdn Bhd, Pahang, Malaysia). It was ground and sieved to obtain a particle size of <36 μm, which became the starting material for membrane fabrication. Reagent-grade chemicals N-methyl-2-pyrrolidone (NMP, QReC™, Kuala Lumpur, Malaysia), polyethersulfone (PESf, Radel A-300, Ameco Performance, Houston, Texas, USA), and Arlacel P135 (polyethyleneglycol 30-dipolyhydroxystearate, CRODA, Snaith, Yorkshire, UK), and tap water were used.

Fabrication of Bauxite-based Hollow-Fiber Membrane (BHFM)

Prior to fabricating the bauxite-based, hollow-fiber membrane (BHFM), ceramic suspensions containing various amounts of bauxite, ranging from 45 to 55 wt.% were prepared by varying the weight of bauxite added to the ceramic suspension.

Bauxite was used as ceramic powder, PES as a polymer binder, and Arlacel P135 as a solvent melted in the oven at 60°C overnight to remove any moisture content in the materials. The suspension solution then was prepared by dissolving Arlacel P135 in NMP. Bauxite was then added to the solution. Dispersion of bauxite in the mixture of Arlacel P135 and NMP was achieved by milling with 10 mm and 20 mm agate mill balls in a planetary ball mill (Model: NQM-2, Magna) at a constant rate of 182 rpm for 48 h to ensure that all elements were well mixed before the polymer binder was added. The milling process was continued for a further 48 h immediately after the addition of PES to allow the polymer binder to dissolve completely in the solution. The formulation of each suspension is tabulated in Table 1.

Upon spinning of the bauxite-based, hollow-fiber (BHFM), the bauxite suspension solution was degassed under vacuum using a magnetic stirrer at the lowest rpm for ~1 h or until no air bubbles were seen on the surface of the suspension. The purpose of this step is to remove completely any air bubbles trapped in the suspension in order to produce well structured hollow fibers. The viscosity of every dope solution was measured using a Brookfield viscometer (Middleboro, Massachusetts, USA). This analysis was required in order to decide whether the prepared suspensions were able to produce the membrane or not because a viscosity which is too low or too high may affect the producibility of the membrane. Prepared bauxite suspensions were then extruded while being spun as stated in Table 2 and the set-up was prepared as illustrated in Fig. 1. The hollow-fiber membranes thus yielded (referred to as precursors) were immersed in the external coagulation bath for ~24 h upon completion of the phase-inversion process.

The precursors were dried at room temperature and then sintered at five different sintering temperatures ranging from 1250 to 1450°C in a tubular furnace (model: XL-1700, Magma, MagmaTherm, Istanbul, Turkey). The sintering process was carried out by increasing the temperature from 50 to 600°C at the rate 2°C/min and held for 2 h, followed by increasing the temperature from 600°C to the target temperature at the rate of 5°C/min and then held for 3 h. The temperature was then reduced from the target temperature to 50°C at the rate of 5°C/min. Upon completing the sintering procedure using the profile as shown in Fig. 2, fabricated BHFM was ready for further analysis.

Table 2. Spinning conditions for the phase-inversion method used to fabricate the bauxite-based, hollow-fiber membranes (BHFM)

Parameter	
Air gap (cm)	5
Extrusion rate (mL/min)	10
Bore fluid rate (mL/min)	9
Internal and external coagulant	Tap water
Tube-in orifice spinneret diameter (mm)	Inner : 1.2 Outer : 2.8

https://doi.org/10.1007/s42860-020-00076-8 Published online by Cambridge University Press

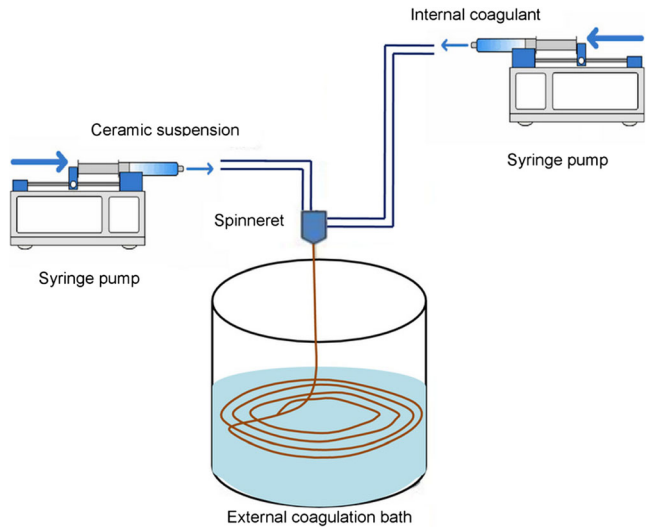

Fig. 1. Schematic diagram of BHFM spinning system (Mohtor 2016)

Rheological Measurement of the Bauxite Suspension

Viscosity analysis is beneficial in finding out the rheological behavior of the mineral suspension before the spinning process and was conducted using a Brookfield AMETEK viscometer (Middleboro, Massachusetts, USA). Shear rates between 1 and 100 s^{-1} were calculated using Eq. 1:

$$\gamma = \left(\frac{2{R_c}^2}{{R_c}^2 - {R_b}^2}\right) \times \omega \quad (1)$$

where γ is the shear rate at the surface of spindle (s^{-1}), R_c is the radius of container (cm), R_b is the radius of spindle (cm), and ω is the angular velocity of spindle (rad/s).

Characterization of Fabricated BHFM

The morphologies of the various BHFM products were observed using an Hitachi TM 3000 scanning electron microscope (SEM) (Hitachi, Tokyo, Japan). The membrane thickness was calculated as the average of three values obtained from the cross-section images (Fig. 5). The BHFM was splintered by forceps to attain a clean-cut cross-section of the membrane which was then placed on a metal holder and sputter-coated with gold under vacuum for 3 min.

The membrane porosity and pore diameter of the BHFM were measured using an Automated Mercury Porosimeter (model: AutoPore™ IV Series, Micromeritics, Norcross, Georgia, USA). Prior to analysis, BHFM was cut into fragments that were fitted in the penetrometer bulb where the total weight of the fragment (with and without the penetrometer) was recorded.

A three-point bending test was conducted to evaluate the mechanical strength of the BHFM by using a tensile tester (model: 3342, Instron, Selangor, Malaysia) with a load cell for 1 kN and the set-up was as per Fig. 3. BHFM was placed on a 43 mm sample holder and a load applied to the membrane. Once fracture occurred, the mechanical strength of the membrane was calculated using Eq. 2.

$$\sigma_f = \frac{8FLD_0}{\pi\left(D_0^4 - D_i^4\right)} \quad (2)$$

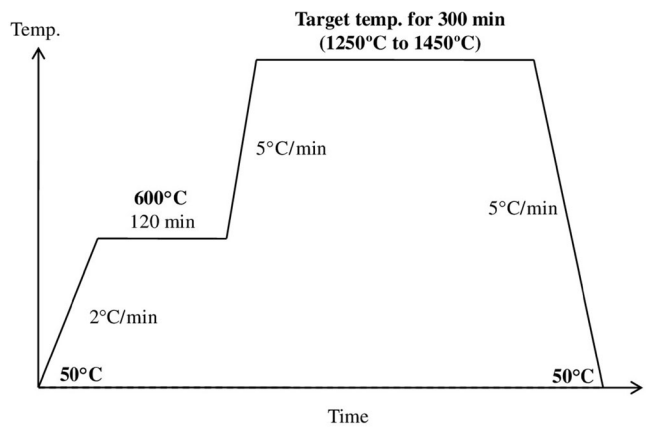

Fig. 2. Sintering temperature profile for BHFM for targeted temperatures of 1250°C, 1300°C, 1350°C, 1400°C, or 1450°C

https://doi.org/10.1007/s42860-020-00076-8 Published online by Cambridge University Press

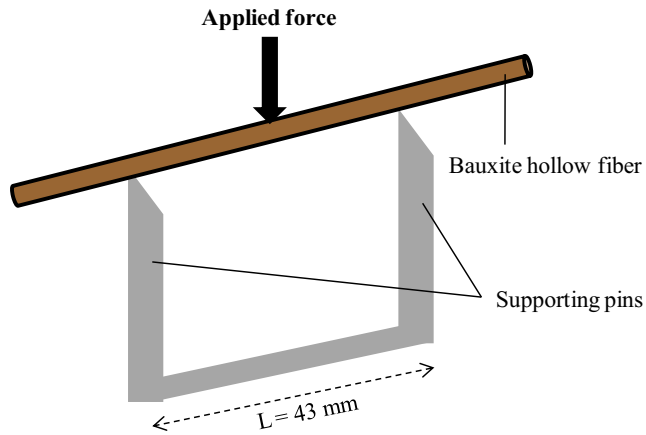

Fig. 3. Schematic diagram of three-point (3P) bending-strength test

where σ_f is the mechanical strength of the membrane (MPa), F is the maximum load required at which the fracture occurred (N), L is the length of membrane (m), D_o is the outer diameter of the membrane (m), and D_i is the inner diameter of membrane (m). The average mechanical strength value was obtained after five measurements were taken.

The water permeability was determined on a ~3–4 cm length of the BHFM using an ultrafiltration device operating in the cross-flow mode at 25°C. The ultrafiltration device was designed and self-assembled using a local fabricator, A critical first step was to saturate the membrane with water at 1.5 bar and allow the reading to stabilize at that pressure (usually ~30 min); then, the pressure was increased to 3 bar and the reading was recorded. The water permability of the membrane was calculated using Eq. 3:

$$L_p = \frac{\Delta V}{A_m \Delta_t \Delta P} \tag{3}$$

where L_p is the water permeation ($L/m^2 \cdot h \cdot bar$), ΔV is the volume of water permeated through the membrane (L), A_m is the effective membrane area (m^2), Δ_t is the permeation time (h), and ΔP is the transmembrane pressure (bar). The average water permeation was measured from three measurements taken for each membrane sample.

Rejection Test on Colored Wastewater

A rejection performance test of the BHFM was carried out using Reactive Black 5 (RB5) with various weights as the synthetic contaminant to be removed. The concentration of RB5 (M_2) was varied from 10 to 30 ppm by diluting a 100 ppm RB5 stock solution with tap water; the dilution factor was given by

$$M_2 = \frac{M_1 V_1}{V_2} \tag{4}$$

where M_1 is the concentration in molarity (mol/L) of the concentrated solution, V_1 is the volume of the concentrated solution, M_2 is the concentration in molarity of the dilute solution (after more solvent has been added), and V_2 is the volume of the dilute solution.

The rejection rate, defined as the fraction of dye removed from solution by the membrane, was calculated using Eq. 5:

$$R(\%) = \left(1 - \frac{C_p}{C_f}\right) \times 100 \tag{5}$$

where R is the fraction of dye rejected (%), C_p is the concentration of dye in the permeate (mg/L), and C_f is the concentration of dye in the feed solution (mg/L).

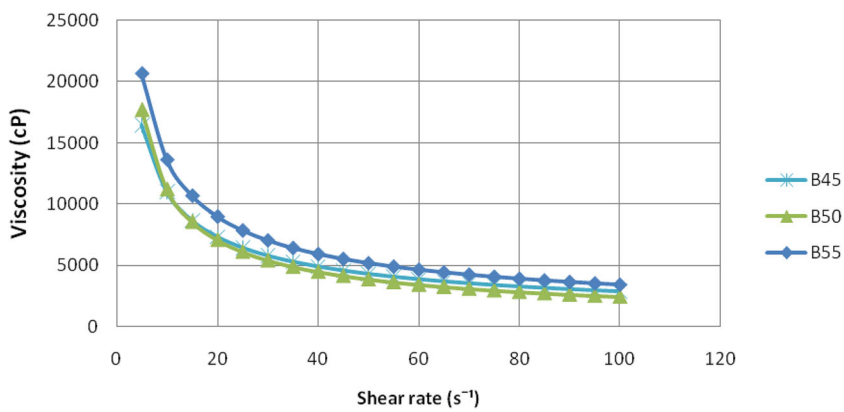

Fig. 4. Rheological behavior of bauxite/NMP/PES/Arlacel suspension solutions prepared with varied bauxite loadings

https://doi.org/10.1007/s42860-020-00076-8 Published online by Cambridge University Press

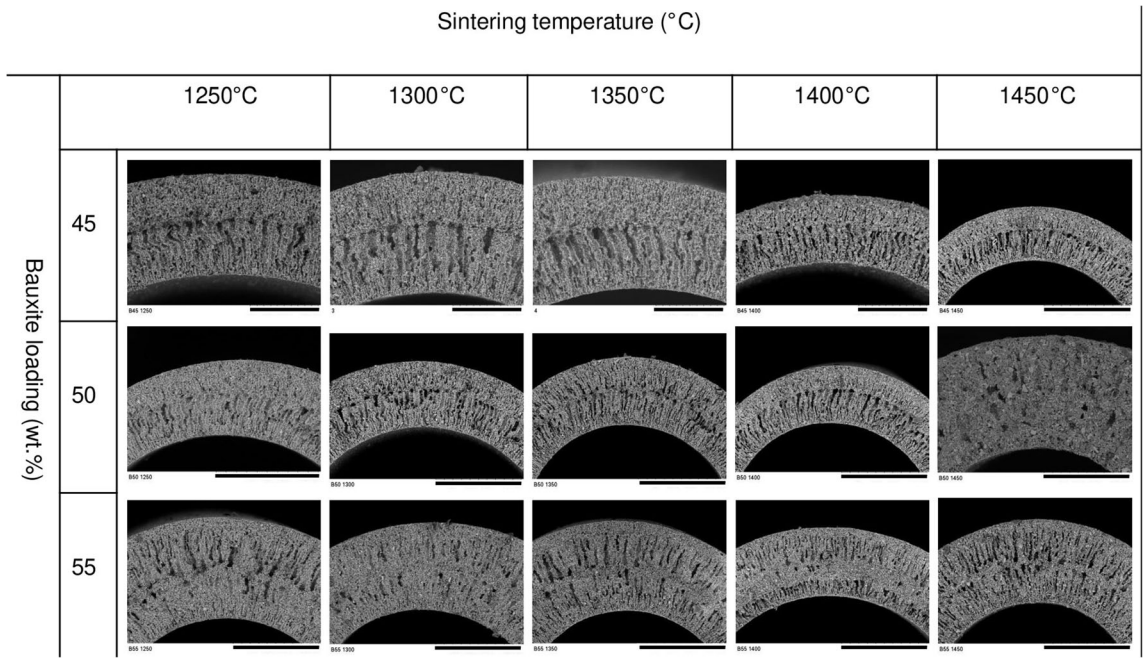

Fig. 5. Microscopic images of BHFM fabricated with various bauxite loadings and sintering temperatures. Scale bars: top row (1–4) – 100 μm; top row (5) and middle and bottom rows – 300 μm

The concentration of the remaining RB5 was determined by measuring the absorbance of colored dye before and after the rejection test using a UV-Vis spectrophotometer (Hach DR5000, Kuala Lumpur, Malaysia) at a wavelength of 597 nm.

RESULTS AND DISCUSSION

Rheological Properties of Bauxite Suspensions

High viscosity is the key property that determines whether the phase-inversion spinning process will produce a continuous hollow fiber from the bauxite precursor. Rheological measurements of 45, 50, and 55 wt.% bauxite loadings (Fig. 4) revealed that 55 wt.% bauxite loading yielded the highest viscosity (7044 cP), and all loadings exhibited shear-thinning flow behavior. The 45 wt.% bauxite suspension had the smallest viscosity (5424 cP) and the viscosity at 50 wt.% was intermediate (5832 cP). According to Ren et al. (2018), the increase in viscosity is due to a decrease in particle mobility. The present findings are in agreement with those of Setz et al. (2012) who reported similar pseudo-plastic flow behavior of alumina powder.

SEM Images

The fabricated BHFM products were analyzed by SEM to determine whether their pore morphologies met the desired structure, i.e. finger-like and sponge-like (Fig. 5). The configuration of 50 wt.% BHFM sintered at 1450°C yielded no finger-like pores, probably due to an inadequate viscosity which hindered development of viscous fingering during the external exchange of phase inversion. Therefore, only some macro voids were seen in the cross-section of the membrane and this finding is parallel to a previous study conducted by Liu and his team (Liu et al. 2003). In contrast, the outer and inner membrane surfaces at various loadings of BHFM (45–55 wt.%), which were sintered at the same temperature, showed identical pore structure with good interconnected pores and uniform pore dispersion without any obvious defects. With increasing sintering temperature, the particles grew in size which led to the decreased porosity.

Table 3. Chemical composition (wt.%) of sintered bauxite

	Chemical composition (wt.%)					
	Al_2O_3	Fe_2O_3	SiO_2	TiO_2	P_2O_5	MnO
Sintered BHFM (this study)	60.60	22.80	11.20	7.21	0.32	0.20
Cao et al. (2014)	63.53	7.08	10.41	2.97	0.22	0.11

https://doi.org/10.1007/s42860-020-00076-8 Published online by Cambridge University Press

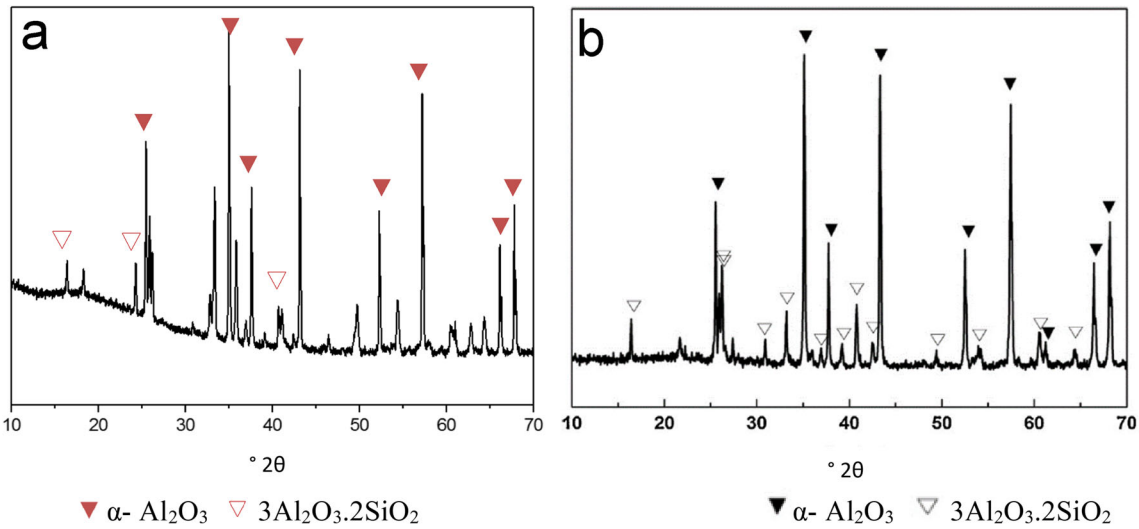

Fig. 6. XRD pattern of **a** sintered BHFM (this study) and **b** sintered BHFM (Li et al., 2016)

In general, however, the electron photomicrographs (Fig. 5) revealed that the phase inversion process (Kingsbury et al. 2010) for membrane fabrication yielded high-quality BHFMs which displayed a uniform configuration and a smooth surface with no apparent cracks, cavities, or irregularities. This unique microstructure was attributed in part to the high suspension viscosity, as this property is essential to prevent the collapse and deformation of partially solidified hollow fibers. On top of that, the colors of the surface of sintered BHFM gradually turned from brownish to dark brown as the sintering temperature increased. The change in color is explained as being due to ferric oxides being incorporated into the lattices of other oxides or when new oxides are formed or phase changes occur at high temperature (Coey et al. 2013).

X-ray fluorescence (XRF) (Axios-Advanced, PANalytical Corporation, Almelo, The Netherlands) and X-ray diffraction (XRD) (X'pert Pro α1, Philips, Amsterdam, The Netherlands) analyses revealed that corundum (Crn - Al_2O_3) is the main oxide (58.6%) in the bauxite used in this study (Table 3 and Fig. 6, respectively), which is comparable to the bauxite used in a previous study by Cao et al. (2014). Other components were hematite (Hem, Fe_2O_3) at 22.8%, quartz (Qz, SiO_2) at 11.20 wt.%, and anatase (Ant, TiO_2) at 7.08 wt.%. Most of the components found in the bauxite were similar though the values are different (in terms of wt.%) from values obtained from bauxites from China (Cao et al., 2014), which indicates that the chemical composition varies depending on geographical origin.

The XRD also identified (Crn – Al_2O_3, hexagonal system, PDF#46-1212) as the major crystalline phase in sintered bauxite (Fig. 6). Mullite (Mul – $3Al_2O_3$•$2SiO_2$, orthorhombic system, PDF#15-0776) was also formed as the sintering processes were conducted, forming by the reaction between corundum (Crn) resulting from the decomposition of diaspore (Dsp) and cristobalite (Crs) from kaolinite (Kln)

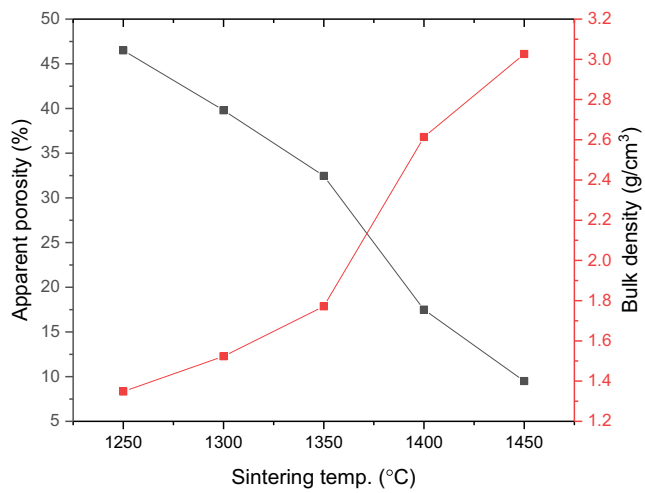

Fig. 7. Bulk density and apparent porosity of BHFM prepared using various sintering temperatures

https://doi.org/10.1007/s42860-020-00076-8 Published online by Cambridge University Press

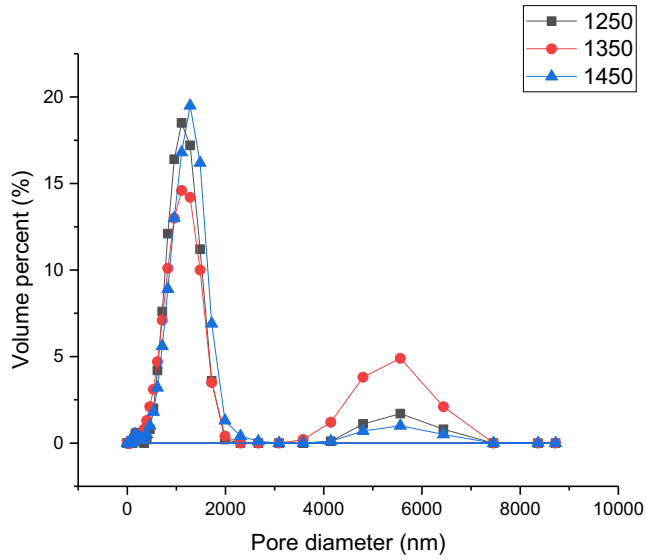

Fig. 8. Pore-size distribution of BHFM sintered at 1250–1450°C

decomposition. This mullite (Mul), a well known classical ceramic material, possessed an excellent chemical and structural stability (Choo et al. 2019).

Apparent Porosity, Bulk Density, and Pore-Size Distribution

A good porous membrane should possess great porosity and excellent mechanical strength. Unfortunately, both of these parameters have a trade-off trend relationship, in which a high mechanical strength membrane has low porosity and vice versa. Larger particles were firmly bridged by the irregular small particles forming the porous structure with good mechanical strength as the hollow-fiber membrane was sintered.

As sintering temperature increased, the bulk density increased and the porosity of the membrane decreased (Fig. 7) from 46.5% in the unsintered material to 9.5% after sintering at 1450°C. For porous ceramics used as separation media, the porosity is often in the range 30–50% (Sarkar and Kim 2015). The BHFM fabricated here at 1350°C and below followed this same pattern. Bulk density is inversely proportional to the porosity and the changes in both confirm that linear shrinkage of the membrane occurs as sintering temperature increases (Sharif et al. 2014).

Any aqueous medium that uses porous ceramics operates mainly through the physical screening process; the separation efficiency and selectivity depend, therefore, on the porosity and pore size. The pore-size distribution of BHFM sintered at 1250°C, 1350°C, and 1450°C (Fig. 8) changed with the variation in sintering temperatures. Pore-size distribution widened and consisted of several peaks, with two major peaks located at ~1500 pm and 5500 pm. At temperatures >1250°C, the average pore size decreased due to the sintering shrinkage of pores. The pore size of sintered BHFMs at 1250–1450°C are suitable for the ultrafiltration membrane in which the pore size must be

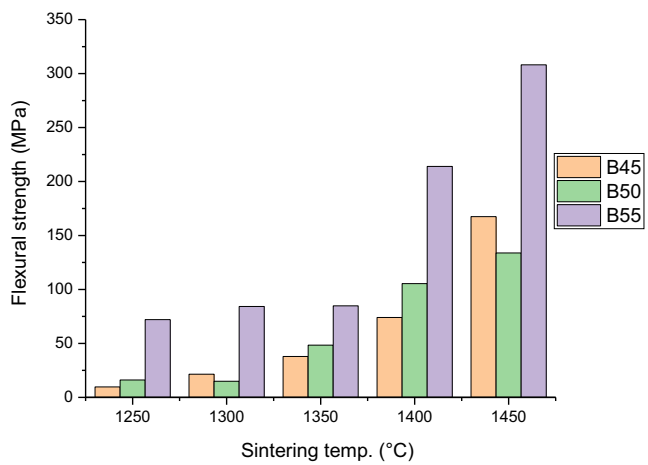

Fig. 9. Mechanical strength of 45, 50, and 55 wt.% BHFM sintered at various temperatures

https://doi.org/10.1007/s42860-020-00076-8 Published online by Cambridge University Press

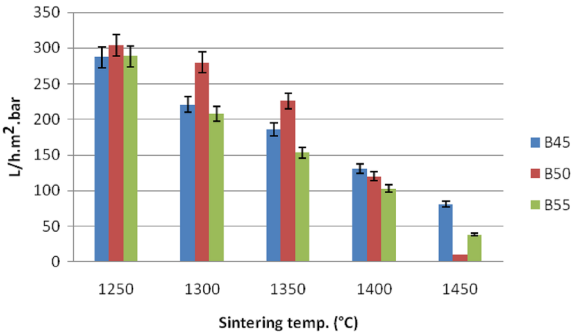

Fig. 10. Pure water flux of BHFM with various bauxite loadings sintered at 1250–1450°C

~2–50 nm (equivalent to 2000–50,000 pm) (Jeon et al. 2016).

Mechanical Strength: Effect of Bauxite Loading and Sintering Temperature

The mechanical strength of BHFMs increased as sintering temperature increased (Fig. 9). This was expected because increased temperature leads to a denser structure caused by a higher diffusion rate (Xiao et al. 2018), and agrees with the findings of Sharif et al. (2014) and Dong et al. (2018).

Increased bauxite loading also increased the mechanical strength of the sintered BHFMs, but all products exceeded the recommended flexural strength of 30 MPa (Silvestre et al. 2015) for porous ceramics as a separation medium. The pressure required to fracture the 1450°C-sintered membrane increased from 156.7 MPa for that loaded with 45 wt.% bauxite to 308.1 MPa for that loaded with 55 wt.% bauxite. In summary, BHFMs fabricated during this study have appropriate flexural strength for typical applications.

Water Permeability: Effect of Bauxite Loading and Sintering Temperature

The permeability to water of the BHFMs sintered at temperatures of >1250°C was less than for those sintered at lower temperatures (Fig. 10). Water permeation was assumed to be inversely proportional to the mechanical strength of the membrane. The BHFM sintered at 1250°C yielded the highest water permeation. Interestingly, no water flux was observed in the 50 wt.% BHFM sintered at the highest temperature of 1450°C due to the densification of the membrane and pore-size shrinkage even though it was quite porous to inhibit the water from flowing through them based on SEM image (based on previous Fig. 7). According to Dong et al. (2018), an increase in sintering temperature might lead to sintering neck formation by diffusion between particles in the BHFM and this finding might be the best explanation for the aforementioned problem. As BHFM becomes denser, the water filtration flow rate slows due to the decrease in pore and water channels for the permeate to go through the membrane.

In terms of bauxite loading, pure water flux (PWF) of the BHFMs from various bauxite contents decreased from 287 L/m^{2}h to 81.38 L/m^{2}h, 304.2 L/m^{2}h to10.0 L/m^{2}h, and 288.64 L/m^{2}h to 38.0 L/m^{2}h with increasing bauxite content from 45 wt.%, 50 wt.%, and 55 wt.% respectively, at the highest and lowest sintering temperature. Increasing the bauxite content decreases the pore size of the fiber structure (Liu and Li 2003) and finger-like voids in the BHFM structure contribute to the high water flux of BHFM (Lawrence and Jiang 2017).

Performance Test of BHFM on RB5 Rejection

Fabricated BHFMs used in the present study rejected or removed up to 99% of the color from RB5-laced wastewater – 50 wt.% loading, 1450°C sintered, and 10 ppm RB5 in the feed solution (Fig. 11). The rejection percentage increased (Fig. 11) with increasing sintering temperature, starting from 57% at 1250°C. This is explained by the pore

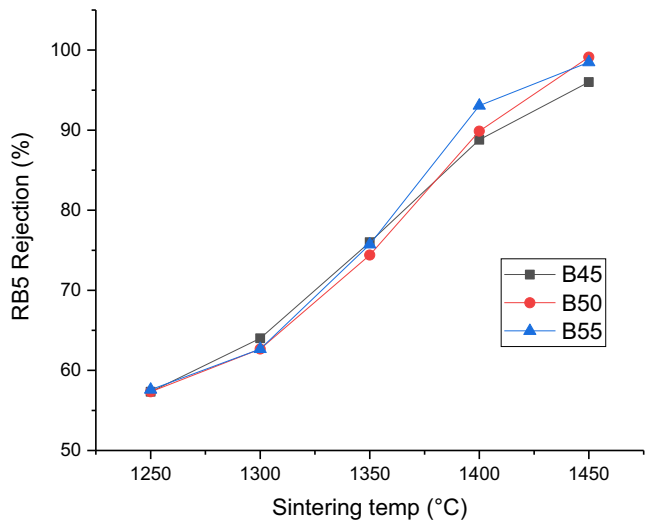

Fig. 11. Rejection test on BHFM for 10 ppm RB5 synthetic wastewater

https://doi.org/10.1007/s42860-020-00076-8 Published online by Cambridge University Press

size and porosity being increasingly larger as the sintering temperature decreases, thus allowing more dye particles to pass through the fabricated membrane (Guillen et al. 2011). As the sintering temperature increased, densification increased and fewer dye particles were able to pass through the BHFM. Nevertheless, even though the removal percentage of RB5 was as low at 57%, this value is still suitable for practical standard applications as it is within the range of permissible effluent limits established by the Interim National Water Quality Standards for Malaysia. The low rejection rate of dye was detected as the lower sintering temperatures were applied to BHFM due to the distribution of larger pore size in the fabricated membrane (Rajput et al. 2016). The porosity of the BHFM also affected the rejection rate as more porous membranes allowed the dye particles to pass through. The bauxite loading did not have a significant influence on the removal of RB5.

CONCLUSION

In this study, asymmetric bauxite, hollow-fiber membranes (BHFM) were developed through phase inversion using raw bauxite powders as the starting material. The properties of the fabricated membranes, as affected by bauxite loading and sintering temperature, were measured. The main results are as follows:

1. Fabricated BHFMs, prepared by spinning in the phase inversion, possess a nearly uniform microstructure resulting from sufficient viscosity in the suspension.
2. BHFM sintered at temperatures ranging from 1250 to 1350°C satisfied the practical application requirements of a separation medium. Their porosities were within the range 30–50% and the flexural strength of all products was > 30 MPa.
3. BHFM exhibited a multi-peak, pore-size distribution with average pore sizes that qualified them to serve as ultrafiltration membranes or membrane supports.
4. The best sintering temperature was 1300 or 1350°C regardless of loading, as the water flux and mechanical strength under these sintering conditions were satisfactory.
5. Among all the membranes fabricated, BHFM sintered at 1300°C possessed optimal properties for all characterizations.

ACKNOWLEDGMENTS

The authors gratefully acknowledge financial support from the Ministry of Education Malaysia under the Higher Institution Centre of Excellence Scheme (Project Number: R.J090301.7809.4J430) and Universiti Teknologi Malaysia under the Transdisciplinary Research Grant (Project number: Q.J130000.3509.05G75), Malaysia Research University Network (MRUN) Grant (Project number: R.J130000.7809.4L867), and UTM Grant Award (Project number: R.J130000.7709.5M003). The authors thank Aras Kuasa Sdn Bhd for the research sample and the Advanced Research Technology Research Centre (AMTEC), Universiti Teknologi Malaysia for the technical support and services provided.

FUNDING

Funding sources are as listed in the acknowledgments.

Compliance with Ethical Statements

Conflict of Interest

The authors declare that they have no conflict of interest.

REFERENCES

Ali, M.S., Ariff, A.H.M., Jaafar, C.N.A., Tahir, S.M., Mazlan, N., Maori, K.A., & Naser, H. (2017). Factors affecting the porosity and mechanical properties of porous ceramic composite materials. In: *Reference Module in Materials Science and Material Engineering*. Elsevier.

Bauxite Index. (2020). https://thebauxiteindex.com/en/cbix/industry-101/bauxite-101/mineralogy/impurities

Bhuiyan, M. A., Hoque, S. M., & Choudhury, S. (2010). Effects of sintering temperature on microstructure and magnetic properties of $NiFe_2O_4$ prepared from nano size powder of NiO and Fe_2O_3. *Journal of Bangladesh Academy of Science, 34*, 189–195.

Cao, J., Dong, X., Lia, L., Dong, Y., & Hampshire, S. (2014). Recycling of waste fly ash for production of porous mullite ceramic membrane supports with increased porosity. *Journal of the European Ceramic Society, 34*, 3181–3194.

Choo, T. F., Salleh, M. A. M., Kok, K. Y., & Matori, K. A. (2019). A review on synthesis of mullite ceramics from industrial wastes. *Recycling, 4*(3), 39.

Coey, J.M.D., Venkatesan, M., & Xu, H. (2013). Introduction to magnetic oxides. Pp. 1–49 in: *Functional Metal Oxides: New Science and Novel Applications* (S.B. Ogale, T.V. Venkatesan, and M.G. Blamire, editors). Wiley, New Jersey.

Dong, L. L., Xiao, B., Liu, Y., Li, Y. L., Fu, Y. Q., Zhao, Y. Q., & Zhang, Y. S. (2018). Sintering effect on microstructural evolution and mechanical properties of spark plasma sintered Ti matrix composites reinforced by reduced grapheme oxides. *Ceramics International*. https://doi.org/10.1016/j.ceramint.2018.06.252.

Ebbesen, S. D., Jensen, S. H., Hauch, A., & Mogensen, M. B. (2014). High temperature electrolysis in alkaline cells, solid proton conducting cells, and solid oxide cells. *Chemical Review, 114*, 10697–10734.

Guillen, G. R., Pan, Y., Li, M., & Hoek, E. M. V. (2011). Preparation and characterization of membranes formed by nonsolvent induced phase separation: a review. *Industrial and Engineering Chemistry Research, 50*, 3798–3817.

Jeon, S., Rajabzadeh, S., Okamura, R., Ishigami, T., Kato, S. H. N., & Matsuyama, H. (2016). The effect of membrane material and surface pore size on the fouling properties of submerged membranes. *Water, 8*, 602–606.

Kingsbury, B. F. K., Wu, Z., & Li, K. (2010). A morphological study of ceramic hollow fiber membranes: a perspective on multifunctional catalytic membrane reactors. *Catalysis Today, 156*, 306–315.

Lawrence, R. & Jiang, Y. (2017). Porosity, pore size distribution, micro-structure. Pp. 39–71 in: *Bio-aggregates Based Building Materials* (S. Amziane and F. Collet, editors). RILEM State-of-the-Art-Reports; Vol. 23. Springer International Publishing, The Netherlands. https://doi.org/10.1007/978-94-024-1031-0_2

Li, L. L., Chen, M. L., & Dong, Y. C. (2016). A low-cost alumina-mullite composite hollow fiber ceramic membrane fabricated via phase inversion and sintering method. *Journal European Ceramic Society*. https://doi.org/10.1016/j.jeurceramsoc.2016.02.020.

Liu, S., & Li, K. (2003). Preparation TiO_2/Al_2O_3 composite hollow fiber membranes. *Journal of Membrane Science, 218*, 269–277.

Liu, S., Li, K., & Hughes, R. (2003). Preparation of porous aluminium oxide (Al_2O_3) hollow fiber membranes by a combined phase-

inversion and sintering method. *Ceramics International, 29*, 875–881.

Ma, H., Yoon, K., Rong, L., Mao, Y., Mo, Z., Fang, D., Hollander, Z., Gaiteri, J., Hsiao, B. S., & Chu, B. (2010). High-flux thin-film nanofibrous composite ultrafiltration membranes containing cellulose barrier layer. *Journal of Materials Chemistry, 20*, 4692–4704.

Meng, Y., Gong, G. H., Wei, D. T., & Yin, Z. (2014). Comparative microstructure study of high strength alumina and bauxite insulator. *Ceramic International, 40*, 10677–10684.

Rajput, H., Verma, A., Kaur, M., Kaur, T. J., & Toor, A. P. (2016). Heterogeneous solar photo-Fenton degradation of reactive Black 5 using foundry sand and fly ash: value addition to waste. *Journal of Environmental Engineering and Landscape Management, 24*, 124–132.

Ren, Q., Li, H., Wu, X., Huo, Z., Hai, O., & Lin, F. (2018). Effect of the calcining temperatures of low-grade bauxite on the mechanical property of mullite ceramics. *International Journal of Applied Ceramic Technology, 15*, 554–562.

Sabbatini, P., Yrazu, F., Rossi, F., Thern, G., Marajofsky, A., & Fidalgo de Cortalezzi, M. M. (2010). Fabrication and characterization of iron oxide ceramic membranes for arsenic removal. *Water Research, 44*, 5702–5712.

Sarkar, N., & Kim, I. J. (2015). *Porous Ceramics*. Intech Open Publication.

Setz, F. L. G., Koshimizu, L., de Mello-Castanho, S. R. H., & Morelli, M. R. (2012). Rheological analysis of ceramics suspensions with high solids loading. *Materials Science Forum, 727–728*, 646–651.

Sharif, N. S. A., Mohamed, J. J., Derita, H. S., Ahmad, Z. A., Abdullah, M. Z., Mohamad, H., & Yusoff, W. A. W. (2014). The effect of sintering conditions on the microstructure and electrical properties of $Pb(Zr_{0.52}Ti_{0.4})O_3$ ceramic. *Journal of Mechanical Engineering and Sciences, 6*, 901–906.

Silvestre, J., Silvestre, N., & de Brito, J. (2015). An overview on the improvement of mechanical properties of ceramics nanocomposites. *Journal of Nanomaterials*. https://doi.org/10.1155/2015/106494.

Xiao, M., Chen, J., Kang, J., Chen, K., Wu, D., & Gao, N. (2018). Effect of heat treatment process on mechanical properties and microstructure of $FeAlCoCrNiTi_{0.5}$ alloy. *AIP Advance, 8*, *095322*.

(Received 27 March 2019; 8 April 2020: AE: Prakash B. Malla)